

NGC 2849 and NGC 6134: two more BOCCE open clusters★

A. V. Ahumada,^{1,2†‡} M. Cignoni,^{3,4} A. Bragaglia,⁴ P. Donati,^{3,4} M. Tosi⁴
and G. Marconi⁵

¹Consejo Nacional de Investigaciones Científicas y Técnicas – CONICET, Argentina

²Observatorio Astronómico de la Universidad Nacional de Córdoba, Laprida 854, 5000, Córdoba, Argentina

³Dipartimento di Astronomia, Università di Bologna, Via Ranzani 1, I-40127 Bologna, Italy

⁴INAF-Osservatorio Astronomico di Bologna, Via Ranzani 1, I-40127 Bologna, Italy

⁵European Southern Observatory (ESO), Alonso de Córdova 3107, Vitacura, Santiago de Chile, Chile

Accepted 2012 December 7. Received 2012 December 7; in original form 2012 October 2

ABSTRACT

We present CCD photometry of two southern open clusters. As part of the Bologna Open Cluster Chemical Evolution project we obtained *BVI* and *UBVI* imaging for NGC 2849 and NGC 6134, respectively. By means of the synthetic colour–magnitude diagram method and using various evolutionary sets of stellar evolution tracks with various metallicities, we determined at the same time age, distance and reddening. We also determined an approximate metallicity for NGC 2849, for which the information is not available from sounder methods like high-resolution spectroscopy. NGC 2849 turned to be 0.85–1.0 Gyr old with a solar metallicity. The foreground reddening is $E(B - V) = 0.28 - 0.32$, and the true distance modulus $(m - M)_0 = 13.8 - 13.9$. For NGC 6134 we did not obtain fully consistent answers from the $V, B - V$ and $V, V - I$ photometry, an unexpected problem, since both the metallicity and the reddening are known (from high-resolution spectroscopy and the $U - B, B - V$ two colours diagram, respectively). This may either indicate a difficulty of current models (evolutionary tracks and/or models of atmosphere) to accurately reproduce colours, or be related to differences in the metal mixture assumed by the models and those of the clusters. Assuming the spectroscopic abundance and the colour excess $[E(B - V) = 0.35]$ from the $U - B, B - V$ plot, we derived a best age between 0.82 and 0.95 Gyr and a distance modulus 10.5. In agreement with previous studies, the NGC 6134 colour–magnitude diagram shows also a clear main sequence gap at $V \sim 15$ and $B - V \sim 0.9 - 1.0$ that is unexplained by canonical stellar evolution models.

Key words: Hertzsprung–Russell and colour–magnitude diagrams – open clusters and associations: general – open clusters and associations: individual: NGC 2849 – open clusters and associations: individual: NGC 6134.

1 INTRODUCTION

It is well known that open clusters (OCs) play a prominent role in the delineation of the chemical and dynamical evolution of the Galactic disc (e.g. Friel 1995). For example, they have been used to determine the Galactocentric metallicity distribution. However, there are some open questions. Some years ago Friel et al. (2002) found an

abundance gradient of -0.06 dex kpc^{-1} over a range in Galactocentric radii (R_{GC}) of 7 to 16 kpc. Twarog, Ashman & Anthony-Twarog (1997) invoked two distributions, at solar ($[\text{Fe}/\text{H}] = 0$) and sub-solar ($[\text{Fe}/\text{H}] = -0.3$) metallicity with a sharp discontinuity at $R_{\text{GC}} \sim 10$ kpc. This feature has recently been attributed to corotation of the gas (e.g. Lépine et al. 2011) that naturally separates inner and outer regions. Recent detailed abundance analyses of OCs up to large R_{GC} seem to favour a negative gradient in the inner region and a flattening in the outer disc (e.g. Sestito et al. 2008; Friel, Jacobson & Pilachowski 2010; Yong, Carney & Friel 2012); however, the systematics between different analyses make impossible to draw firm, definitive conclusions. The situation is even more complicated if we consider other disc tracers, like cepheids, young stars or planetary nebulae, and the effect of radial mixing (to which OCs seem however less subject, see e.g. Wu et al. 2009).

★This work is based on observations made at the ESO telescopes in La Silla (Chile) under programmes 59.E-0532 and 67.D-0014.

†E-mail: andrea@oac.uncor.edu

‡This work was done while AVA was an ESO Fellow hosted at INAF-Osservatorio Astronomico di Bologna, Italy.

Part of the mentioned differences in the obtained results are due to the lack of homogeneity in the analysed data taken from diverse sources. With the aim to resolve that point the ‘Bologna Open Cluster Chemical Evolution’ (BOCCE) project was started (see Bragaglia & Tosi 2006 for a description of method and goals). One of the goals of this long-term project is to build a homogeneous sample of OCs large enough to be representative of the whole OC population. By means of photometry and synthetic colour-magnitude diagrams (CMDs), age, distance, reddening and a first indication of metallicity are derived at the same time. Medium- and high-resolution spectroscopy are used to derive radial velocities and chemical abundances, respectively (see e.g. Bragaglia et al. 2001, 2006). For the clusters in common, metallicities will also be adopted from ongoing large-scale surveys, like the Apache Point Observatory Galactic Evolution Experiment (APOGEE; Majewski 2012) or the *Gaia* European Southern Observatory (ESO) Survey (Gilmore et al. 2012) – of which some of the authors are members – taking care of homogenization. We presently have data for about 50 OCs, and we have published results based on photometry for about half of the sample (see Cignoni et al. 2011; Donati et al. 2012, and references therein). Here we present part of our last effort, concerning the photometric data obtained for two austral intermediate age OCs: NGC 2849 and NGC 6134.

NGC 2849, also known as Cr 207 (Collinder 1931), ESO 314-SC013 (Lauberts 1982) or Lund 499 (Lyngå 1987), is a relatively compact cluster with an apparent diameter of ~ 3 arcmin, classified as Trumpler class I 1m according to the Lyngå Catalogue (Lyngå 1987). It is located in the third Galactic quadrant in the Vela constellation ($l = 265^\circ 27'$, $b = +6^\circ 36'$). The first CCD *BVI* study was carried out by Ahumada (2003), who obtained by means of solar isochrones fitting a reddening range $0.46\text{--}0.57$ (± 0.12 mag), a distance modulus $(m - M)_0 = 14.02 \pm 0.40$ and an age $\log(t) = 8.8 \pm 0.1$. More recently, Kyeong et al. (2004) by means of multi-band *UBVIJHK* photometry, found for this OC a colour excess $E(B - V) = 0.50 \pm 0.04$ and a metallicity $[\text{Fe}/\text{H}] = -0.24 \pm 0.12$ determined from the ultraviolet excess. Fitting the zero age main sequence they obtained $(m - M)_0 = 13.93 \pm 0.17$, and an age of $\log(t) = 8.8 \pm 0.1$ from sub-solar isochrones fitting.

NGC 6134 belongs to the Trumpler class II 3m with an apparent diameter of 6 arcmin (Lyngå 1987). It is located near the Galactic plane in the Norma constellation, at less than 26° from the Galactic Centre direction ($l = 334^\circ 92'$, $b = -0^\circ 20'$). Also known as Cr 303 (Collinder 1931), Melotte 146 (Melotte 1915) and BH 191 (van den Bergh & Hagen 1975), NGC 6134 is a well-studied OC. The first photometric study was carried out by Lindoff (1972) who derived, by means of *UBV* photometry, a colour excess $E(B - V) = 0.45$, a distance of ~ 700 pc and an age near 0.7 Gyr. Based on *UBV* CCD data for stars located at the centre of the cluster, Kjeldsen & Frandsen (1991) determined a reddening $E(B - V) = 0.46 \pm 0.03$, $(m - M)_0 = 9.80$ and an age $\log(t) = 8.95$. By means of CORrelation RADial VELOCITY (CORAVEL) radial velocity measurements and photometry in the *UBV* and Washington system of 24 red giants, supplemented by David Dunlap Observatory (DDO) system observations of 11 stars in the field of NGC 6134, Clariá & Mermilliod (1992) identified 17 red giant members and six spectroscopic binaries. From the photometric analysis they obtained a reddening $E(B - V) = 0.35 \pm 0.02$ and a distance of about 760 pc; from the UV excesses they derived a low metallicity value ($[\text{Fe}/\text{H}] = -0.05 \pm 0.12$). Bruntt et al. (1999) analysed Strömgren photometry and determined an interstellar reddening $E(b - y) = 0.263 \pm 0.004$ (which translates to $E(B - V) = 0.365$, according to Cousins & Caldwell 1985), $[\text{Fe}/\text{H}] = 0.28 \pm 0.02$; they found an age of

0.69 ± 0.10 Gyr from isochrone fitting. From *BVRI* CCD observations, Ahumada (2002) determined a colour excess range: $0.29 \leq E(B - V) \leq 0.37$, an age $\log(t) = 9.1$ and a distance of about 1080 ± 50 pc. Frandsen et al. (1996) found at least six δ Scuti stars using differential photometry, while Paunzen & Maitzen (2002), by means of Johnson and Strömgren photometric measurements, found five variable objects within the field of NGC 6134. Rasmussen et al. (2002) determined the rotational velocities of them and of several other non-variable stars in NGC 6134. They carried out an abundance analysis of the δ Scuti stars to confirm the high metal content of this cluster: $[\text{Fe}/\text{H}] = 0.38 \pm 0.05$. Smiljanic et al. (2009) derived, by means of spectra of high resolution, abundances of Na, C, N and O, and the $^{12}\text{C}/^{13}\text{C}$ ratio in a sample of three giant stars members of NGC 6134. From high-resolution spectra, Carretta et al. (2004) derived iron abundances, finding $[\text{Fe}/\text{H}] = 0.15 \pm 0.03$ and a colour excess $E(B - V) = 0.355 \pm 0.005$, while Mikolaitis et al. (2010) determined abundances of several chemical elements using the same spectra.

In Section 2, we present our new photometric data and the procedures to perform the data reduction. We present in Section 3 the CMDs and in Section 4 the clusters’ parameters derivation. A discussion and the conclusions of the present study are summarized in Section 5.

2 OBSERVATIONS AND DATA REDUCTION

NGC 2849 was observed on 1997 May 10 with the 0.91 m Dutch telescope, located at the La Silla Observatory (ESO, Chile). The TK512CB CCD Tektronix of 580×520 pixels was mounted at the direct camera. The CCD operated with a gain of $3.6 \text{ e}^- \text{ ADU}^{-1}$ and a readout noise of 7 e^- . One pixel corresponds to 0.44 arcsec on the sky, so the observed field was 4.2×3.8 arcmin 2 . The filters used were *B* (ESO#419), *V* (ESO#420) and *I* (ESO#465). We observed the centre of the cluster (FC) and a region (FN) located ~ 2 arcmin to the north of FC (see Fig. 1). Seeing values during the observations were from 0.97 to 1.36 arcsec; both FC and FN were observed with airmass values less than 1.45. We also observed standard stars from Landolt (1992) to calibrate the instrumental magnitudes to the standard system. PG0918+029 and PG1323–086 were observed before and after the cluster observations.

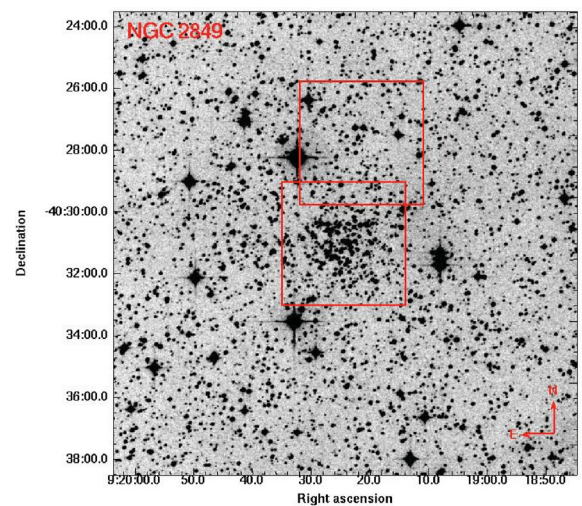


Figure 1. DSS image of the centre of NGC 2849 (FC) and a region at the north (FN). The red squares indicate the observed zones. The map is 15 arcmin \times 15 arcmin. North is up and east is left.

Table 1. Journal of observations for the clusters centres and their external fields. The exposure times (T) are in seconds (s).

Cluster	α_{2000} (h:m:s)	δ_{2000} (°:′:″)	Date	Telescope	T_U (s)	X_U	T_B (s)	X_B	T_V (s)	X_V	T_I (s)	X_I
NGC 2849 _{FC}	09:19:23	−40:31:04	1997 May 10	Dutch	—	—	60	1.040	60	1.091	30	1.144
					—	—	1200	1.076	600	1.122	600	1.156
NGC 2849 _{FN}	09:19:20	−40:28:05	1997 May 10	Dutch	—	—	60	1.339	60	1.246	60	1.398
					—	—	1200	1.296	600	1.371	600	1.449
NGC 6134	16:27:45	−49:09:47	2001 May 15 (N1)	Danish	10	1.110	2	1.121	1	1.124	2	1.130
					30	1.118	5	1.140	2	1.127	5	1.134
					—	—	10	1.162	5	1.138	10	1.185
					—	—	30	1.145	10	1.199	30	1.234
					—	—	—	—	30	1.210	—	—
		2001 May 16 (N2)	Danish	300	1.075	300	1.099	180	1.136	30	1.063	
					900	1.068	600	1.079	300	1.214	180	1.142
					—	—	—	—	600	1.106	300	1.162
NGC 6134 _{Ext}	16:27:51	−49:48:41	2001 May 15 (N1)	Danish	—	—	60	1.080	60	1.078	10	1.082
					—	—	900	1.070	600	1.070	60	1.077
					—	—	—	—	—	—	600	1.075

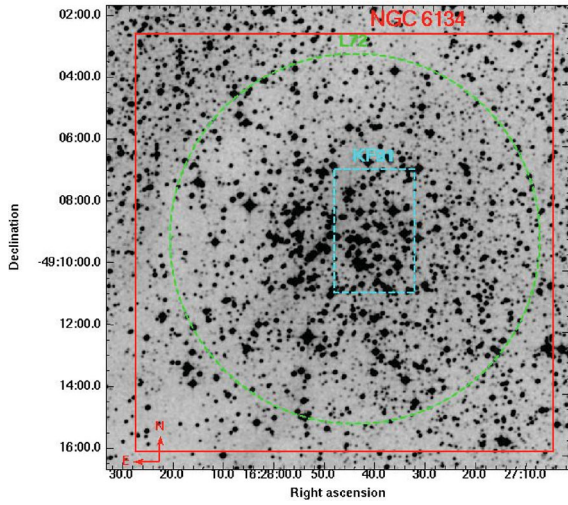
**Figure 2.** DSS image of NGC 6134. The red square indicates the field observed by us, the dashed cyan square indicates the field observed by Kjeldsen & Frandsen (1991) and the green circle indicates the field observed by Lindoff (1972). The map is 15 arcmin \times 15 arcmin. North is up and east is left. The external field, not shown here, is about 40 arcmin south of the cluster centre.

Table 1 shows the log of observation for both clusters. The first five columns indicate the designation of the clusters, equatorial coordinates, observation date and telescope used, while the other ones indicate exposure time in seconds (T) for each filter and the corresponding airmass (X).

In Fig. 2, we present the observed region of NGC 6134. It was observed on 2001 May 15–16 with the Danish Faint Object Spectrograph and Camera mounted at the Danish 1.54 m telescope, La Silla Observatory (ESO, Chile). The detector was a CCD MAT/EEV with 2148×2102 pixels. The observations were performed with a readout noise level of 3.1 e^- and a gain of $0.74 \text{ e}^- \text{ ADU}^{-1}$. The pixel scale of $0.39 \text{ arcsec pix}^{-1}$ permitted a field of $14.0 \times 13.7 \text{ arcmin}^2$. The observations were taken with the filters U (ESO#632), B (ESO#450), V (ESO#451) and I (ESO#425). Despite the poor seeing values (~ 2 to $\sim 3 \text{ arcsec}$) during the first night (N1), we also observed an external field (Ext) distant $\sim 40 \text{ arcmin}$ from the cluster centre to be used for comparison and field fore/background contamination. The second night (N2) was photometric and seeing values

ranged from 1.1 to 1.4 arcsec. All the observations were obtained with airmasses lower than 1.22 as we see from Table 1. To calibrate instrumental magnitudes to the standard system we observed two regions from Landolt’s (1992) list: PG1323–086 and PG1657+078 before the cluster.

2.1 Reduction and photometric calibration

Bias and twilight sky flats for every filter were taken. The data reduction was done with IRAF¹ in the standard way: we applied bias subtraction and flat fielding to all images, with weighted combined calibration frames, and the images were trimmed. For the clusters and their external fields we constructed the point spread function (PSF) determined from well-isolated stars in each frame, using fitting routines in the DAOPHOT/ALLSTAR series of programs of Stetson (1987). Aperture corrections were calculated with aperture photometry of about 10 isolated stars in the reference image per filter to bring the PSF magnitudes on the same scale of the aperture magnitudes of the standard stars. The aperture corrections found for NGC 2849 were -0.02 in B , -0.03 in V and -0.04 in I ; for NGC 6134 we found -0.04 for U , -0.06 for B , -0.03 for V and -0.13 for I . The PSF photometry was finally aperture corrected, filter by filter.

Following IRAF standard procedures, we derived the instrumental magnitudes for the standard stars from aperture photometry and the transformation equations between instrumental and standard magnitudes for each cluster. The magnitudes of standard stars ranged from $V \sim 12$ to $\sim 14.5 \text{ mag}$, while the range for $B - V$ and $V - I$ was ~ -0.3 to $\sim 1.0 \text{ mag}$. We obtained the following set of equations for NGC 2849:

$$B(b, B - V) = b - 3.33 - 0.23 \cdot X_b + 0.074 \cdot (B - V)$$

$$V(b, B - V) = v - 2.97 - 0.13 \cdot X_b + 0.02 \cdot (B - V)$$

$$V(v, V - I) = v - 2.92 - 0.17 \cdot X_v + 0.02 \cdot (V - I)$$

¹ IRAF is distributed by the National Optical Astronomy Observatory, which is operated by the Association of Universities for Research in Astronomy (AURA) under cooperative agreement with the National Science Foundation.

$$I(v, V - I) = i - 4.07 - 0.05 \cdot X_i + 0.004 \cdot (V - I),$$

where b , v and i are the instrumental magnitudes and B , V and I are the calibrated ones. The mean difference between V determined from $(V - I)$ and V determined from $(B - V)$ is 0.0039 ± 0.0033 mag. The equations were obtained with an rms range from 0.009 to 0.021, while the coefficient errors were from 0.004 to 0.01. Uncertainties on calibrated magnitudes and colours were obtained by propagating the different errors involved in the transformation equations. For NGC 2849, the independent instrumental magnitudes were all combined using the stand-alone DAOMATCH and DAOMASTER programs, kindly provided by Stetson (1993).

As mentioned before, for NGC 6134 only N2 was photometric, and we obtained the transformation equations presented below, with an rms range from 0.014 to 0.021. The V magnitudes of standard stars ranged from ~ 12 to ~ 15.3 mag, while the range for the colours were $B - V$ and $V - I$ from ~ -0.3 to ~ 1.0 mag and $U - B$ from -0.08 to 0.52 mag. The errors involved in the determination of the coefficients were on average ~ 0.05 ,

$$U(b, U - B) = u - 2.76 - 0.42 \cdot X_u + 0.07 \cdot (U - B)$$

$$B(b, U - B) = b - 0.58 - 0.08 \cdot X_b + 0.08 \cdot (U - B)$$

$$B(b, B - V) = b - 0.61 - 0.10 \cdot X_b + 0.10 \cdot (B - V)$$

$$V(b, B - V) = v - 0.34 - 0.01 \cdot X_v + 0.01 \cdot (B - V)$$

$$V(v, V - I) = v - 0.34 - 0.01 \cdot X_v + 0.01 \cdot (V - I)$$

$$I(v, V - I) = i - 1.66 + 0.04 \cdot X_i - 0.02 \cdot (V - I).$$

We combined all the independent instrumental measurements of NGC 6134 using the CATAXCORR and CATACOMB programs, kindly provided by P. Montegriffo. Since N1 was not photometric, we calibrated the corresponding data using N2 observations. To calibrate the instrumental magnitudes of the external field to the standard system, since there are no stars in common, we simply shifted in colour and magnitude the resulting CMD, until the same features visible in the central CMD were matched. Since the external field is only used to better define the field contamination, we deemed this approach sufficient.

The final catalogue obtained for each cluster consists of a running number per star (ID), the x and y coordinates, RA and Dec., standard magnitudes and colours, and their instrumental errors. Equatorial coordinates were obtained transforming pixel positions by means of CATAXCORR and the Guide Star Catalogue-II (GSC II). The catalogue for NGC 2849 (FC and FN) contains 1157 stars, of which 820 have B , V and I magnitudes, 836 B and V magnitudes, and 1124 V and I magnitudes. For NGC 6134 the catalogue contains 6623 stars; 1639 present U , B , V and I magnitudes, 1718 present U and B magnitudes, 4067 present B and V magnitudes, and 6534 present V and I magnitudes. These tables will be available only in electronic form through the WEBDA² data base and the CDS portal.³

2.2 Completeness analysis

The completeness of our photometry for both clusters was derived using the usual method of artificial stars (see e.g. Donati et al. 2012

Table 2. Completeness for NGC 2849 in the BVI filters.

Magnitude	Completeness V		Completeness B		Completeness I	
	FC	FN	FC	FN	FC	FN
15.5	0.980	0.994	0.974	1.000	1.000	1.000
16.5	0.974	0.994	0.980	0.990	0.959	0.990
17.5	0.957	0.983	0.977	0.983	0.958	0.996
18.5	0.947	0.963	0.952	0.974	0.928	0.968
19.5	0.905	0.946	0.939	0.968	0.862	0.910
20.5	0.857	0.905	0.894	0.935	0.658	0.796
21.5	0.620	0.724	0.743	0.867	0.240	0.300
22.5	0.226	0.306	0.390	0.470	0.020	0.030
23.5	0.023	0.021	0.044	0.077	0.000	0.000
24.5	0.000	0.000	0.001	0.001	0.000	0.000

for a recent description), i.e. creating the luminosity function on the longest exposure frame for each filter and adding 20 000 and 40 000 artificial stars to NGC 2849 and NGC 6134, respectively. The procedures add and distribute only a fraction of the artificial stars, repeating the tasks as many times as needed to reach the requested number; this is done to avoid introducing additional crowding or local effects. All the data reduction was done as in the real case, as described in previous papers of the BOCCE project (e.g. Tosi et al. 2004 for detailed discussion). Table 2 shows the completeness factor for the FC and FN regions of NGC 2849, while Table 3 shows that for NGC 6134 and its external field. For magnitudes brighter than 15.5 mag, the completeness is 100 per cent.

2.3 Comparison with other data

We can compare our photometry with those obtained by other authors. For NGC 2849 we checked our BVI data with the Ahumada (2003) and Kyeong et al. (2004) ones, as we can see in Figs 3 and 4. The V magnitudes derived by us are very similar to the Ahumada (2003) and Kyeong et al. (2004) ones, while for B and I magnitudes there are little offsets. The average differences are small, so our NGC 2849 photometry is in reasonable concordance with the other existing ones.

In the case of NGC 6134 we compared stars of our sample with the few Clariá & Mermilliod (1992) data, at least for the V magnitudes and the colour indices $(B - V)$ and $(U - B)$ (see Fig. 5). The agreement is very good, as shown by the very small offsets and the absence of trends. When we compare our photometry to the V and $B - V$ data by Kjeldsen & Frandsen (1991) (see Fig. 6) the agreement is worse for $B - V$ data. This could be due either to our photometry or to theirs, but we are more inclined towards the latter possibility, given the fair agreement found with Clariá & Mermilliod (1992). Furthermore, if we compare our V data with the Strömgren y (V Johnson and y Strömgren have similar central wavelengths) by Bruntt et al. (1999), we find again a reasonable agreement (see Fig. 7). We can then conclude that the quality of our calibration is more than acceptable.

3 COLOUR-MAGNITUDE DIAGRAMS

A more detailed discussion of the evolutionary sequences and the properties of both clusters can be found in the next sections. We present here a short description of the main features.

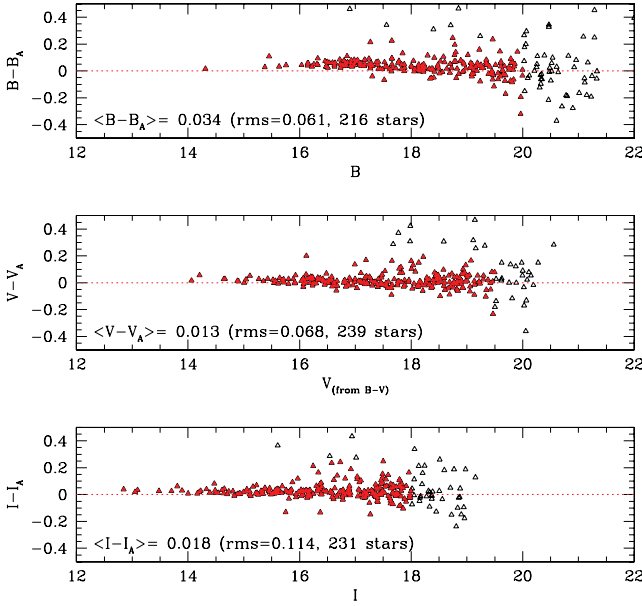
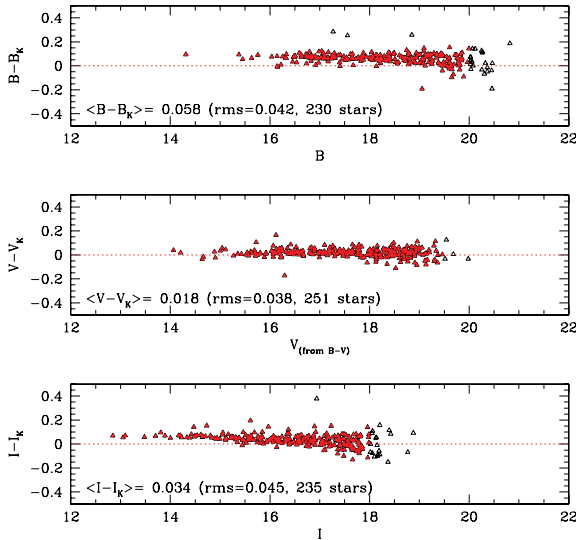
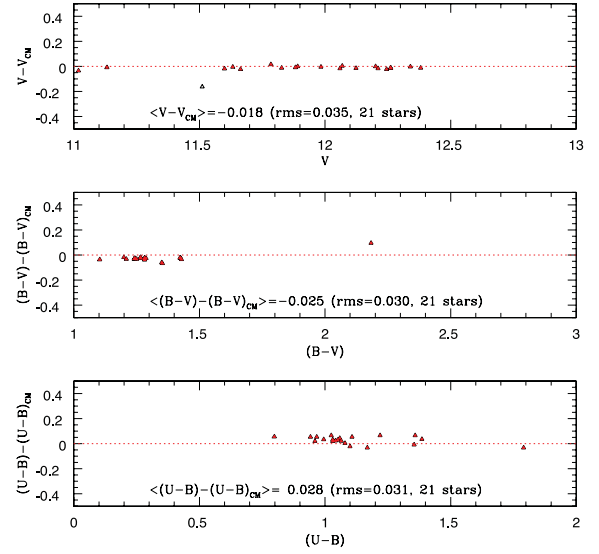
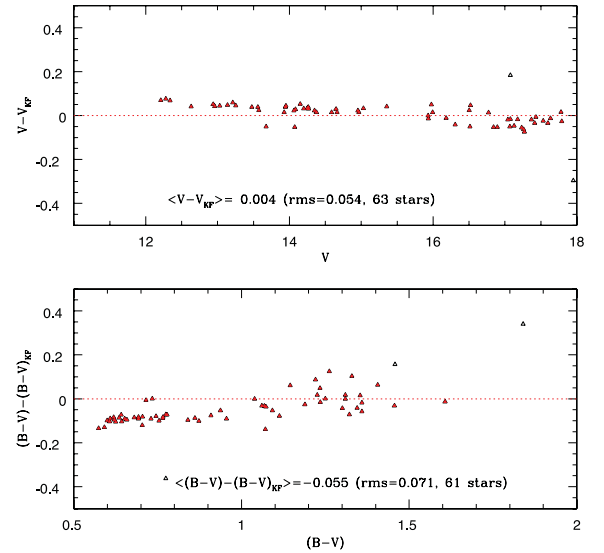
Fig. 8 shows the $V, B - V$ and $V, V - I$ diagrams for the centre of NGC 2849 (FC, upper panels) and for the more external field (FN, lower panels). We see that V reaches as deep as 22 mag, and for FC the main sequence (MS) and the turn-off (TO at $V \sim 15.8$,

² <http://www.univie.ac.at/webda/>

³ <http://cds.u-strasbg.fr/>

Table 3. Completeness for NGC 6134 and its external field in the different filters.

Magnitude	Completeness <i>U</i> Cluster	Completeness <i>B</i> Cluster	Completeness <i>V</i> Ext	Completeness <i>V</i> Cluster	Completeness <i>V</i> Ext	Completeness <i>I</i> Cluster	Completeness <i>I</i> Ext
15.5	0.995	1.000	1.000	1.000	1.000	0.972	1.000
16.5	0.996	1.000	1.000	1.000	0.973	0.954	1.000
17.5	0.988	0.989	0.973	0.966	0.920	0.907	0.996
18.5	0.980	0.970	0.945	0.955	0.871	0.815	0.799
19.5	0.966	0.973	0.910	0.914	0.765	0.604	0.558
20.5	0.860	0.932	0.824	0.863	0.609	0.144	0.277
21.5	0.252	0.889	0.698	0.723	0.371	0.008	0.059
22.5	0.002	0.637	0.375	0.261	0.088	0.000	0.011
23.5	0.000	0.075	0.043	0.009	0.005	0.000	0.000
24.5	0.000	0.004	0.004	0.000	0.000	0.000	0.000

**Figure 3.** Comparison of our *BVI* photometry of NGC 2849 and the one derived by Ahumada (2003). Stars indicated by red triangles were used to determine the average differences and their rms. The number of selected stars are also indicated.**Figure 4.** Same as in Fig. 3, but the comparison is with the Kyeong et al. (2004) *BVI* photometry.**Figure 5.** Comparison for NGC 6134 with *V*, *B - V* and *U - B* data from Clariá & Mermilliod (1992).**Figure 6.** Comparison between our *V* photometry of NGC 6134 and *V* and *B - V* data from Kjeldsen & Frandsen (1991). Stars indicated by red triangles were used to determine the average differences and their rms. The number of selected stars are also indicated.

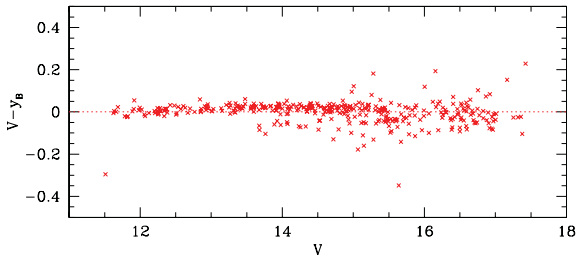


Figure 7. Comparison between our Johnson V and y Strömgren of Bruntt et al. (1999) for NGC 6134.

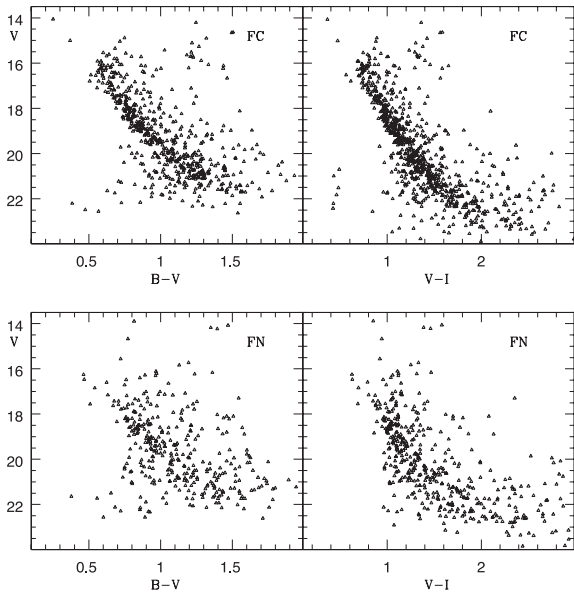


Figure 8. $V, B - V$ and $V, V - I$ CMDs for NGC 2849 (FC, upper panels) and the northern field (FN, lower panels).

$B - V \sim 0.6$, $V - I \sim 0.9$) are clearly visible. To better discriminate between cluster and field stars, in Fig. 9 we present $V, B - V$ CMDs for different radial distances for FC and FN stars. In the external part we see what seems the main sequence of field disc stars, without a clear TO or evolved stars, while for the inner regions the CMD structure of the OC is clearly visible, with a defined MS, TO and a red clump (RC).

For NGC 6134, Fig. 10 presents $V, B - V, V, V - I$ and $U, U - B$ diagrams for the cluster (upper panels); for the external field we only present two CMDs: $V, B - V$ and $V, V - I$ (lower panels). In the upper panels we see not only a very well defined MS extending as deep as $V \sim 22$, but also the RC near $V = 12$, $B - V = 1.4$ and $V - I = 1.7$. We see that for $V \leq 13$ mag the external field (lower panels) is practically empty, and for $V \leq 15$ mag the external CMD is scarcely populated. In Fig. 11, we plot the CMD of NGC 6134 for subregions with different distances from the cluster centre. As usual, the main evolutionary features are better delineated in the inner regions, but the cluster is still evident at about 7 arcmin from its centre.

In the external field of NGC 6134 (Fig. 10), we see another sequence from $V \sim 20$, $B - V \sim 3.2$ to $V \sim 14$, $B - V \sim 2.0$, parallel to the MS. This sequence is due to the population of the disc, and in particular to RC stars at different distances and/or reddening (see e.g. Cignoni et al. 2008). One can immediately appreciate the different behaviour of this feature in the central and comparison fields; unfortunately we seem to have chosen a line of

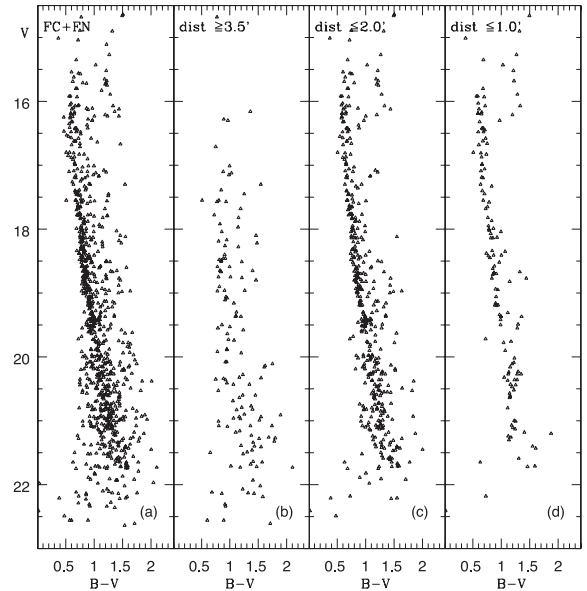


Figure 9. Radial $V, B - V$ diagrams for NGC 2849. FC and FN stars (a). Stars in the external part, with distances ≥ 3.5 arcmin (b); distances ≤ 2.0 arcmin (c); distances ≤ 1.0 arcmin (d). The centre of the stars distribution is assumed as the FC centre.

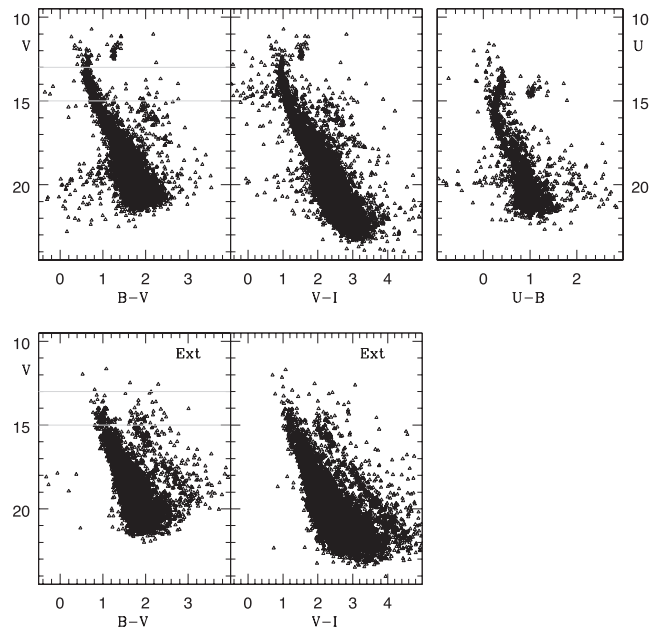


Figure 10. $V, B - V$ and $V, V - I$ CMDs for NGC 6134 (upper panels) and an external field (Ext, lower panels). The $U, U - B$ diagram is shown only for the cluster due to the absence of U data for the external field.

sight with somewhat different properties from the cluster's. Fortunately, this is true only for the fainter magnitudes; TO and RC are well constrained and the comparison to synthetic models is not hampered.

Another exotic feature of this cluster appears in the radial CMDs of Fig. 11. The central part of the cluster, i.e. for radii smaller than 2.0 arcmin, shows a striking MS gap at $V \sim 15$, $B - V \sim 0.9-1.0$, which partially disappears moving outwards. This gap is not a result of mismatches in our photometry. It was first detected by Kjeldsen & Frandsen (1991), who also discussed a similar case in the intermediate age OC IC 4651. The gap is a genuine cluster feature,

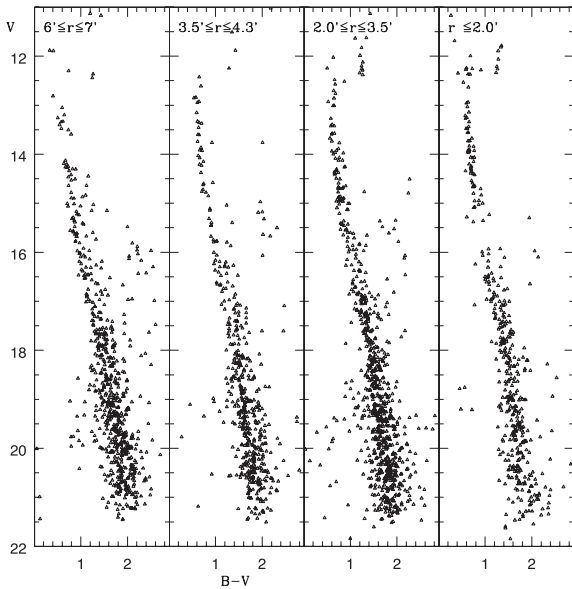


Figure 11. $V, B - V$ diagrams for NGC 6134 in consecutive annular regions of approximately equal area around the adopted cluster centre.

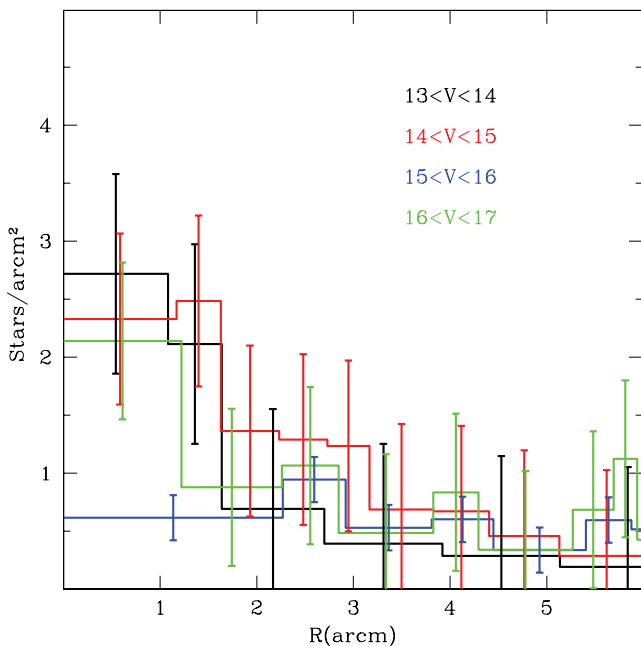


Figure 12. Radial profiles of NGC 6134 MS stars for the labelled ranges of magnitude. The blue line (in the online article) represents the radial distribution of MS stars in the magnitude range of the gap. 1σ error bars are shown.

masked at larger radii by the proportionally increasing contamination by foreground and background stars. This is revealed more clearly by Fig. 12 which shows the radial profiles of MS stars for different ranges of magnitude. In the plot each radial bin contains the same number of stars, i.e. 10. Within 3–4 arcmin from the cluster centre the profile (blue line) corresponding to the stars with the gap magnitude lies systematically below the other profiles, while it is at the same level for the outer stars. Moreover, its overall trend is flat, suggesting that this magnitude range is dominated by field stars rather than cluster stars. The statistical significance of the gap is about 2σ .

Similar gaps have been found also in very well studied systems, but their detection has been often complicated by low-number statistics, completeness issues and field contamination. For instance, de Bruijne, Hoogerwerf & de Zeeuw (2000) identified two gaps at $B - V \sim 0.38$ and ~ 0.48 in the MS of the Hyades, an OC with age and metallicity similar to NGC 6134 (about 0.7 Gyr, $[\text{Fe}/\text{H}] = +0.17$, and negligible reddening according to the WEBDA). The redder gap had also been noted before by Böhm-Vitense (1995). D’Antona et al. (2002) could explain the bluer gap adopting the full spectrum of turbulence (FST; Ventura et al. 1998) model tracks to simulate the Hyades; but they found that another explanation is needed for the redder gap. Furthermore, Subramaniam & Bhatt (2007) found an indication of an MS gap at $(B - V)_0 \sim 0.38$ in the young (400 Myr) cluster NGC 7245 and Giorgi et al. (2002) found a pronounced gap in the very young (50 Myr) OC NGC 2571 at $0.15 < (B - V)_0 < 0.25$ demonstrating that this gap is not produced by a random process but is a real lack of stars in a given magnitude interval. Balaguer-Núñez, Jordi & Galadí-Enríquez (2005) applied a significance test to several OCs with evidence of multiple MS gaps, namely NGC 2548, Pleiades, Hyades, NGC 1817 and M67, finding no clear correlation with age and metallicity. The same authors suggested that all these gaps could be classified into four main loci with colours $(B - V)_0 \sim 0.3, 0.4, 0.7, 0.9$, respectively.

Among field stars, the existence of MS gaps is still debated. Using very precise temperatures (computed from line depth ratios) for 248 F-K field dwarfs of about solar metallicity with *Hipparcos* parallaxes, Kovtyukh, Soubiran & Belik (2004) found a gap at $(B - V)_0 \sim 0.7$ (which is close, but not identical, to the locus of our gap). Interestingly, the authors noted that this gap is located near the hot edge of the lithium depression (where lithium is depleted by orders of magnitude) in field dwarfs, with dwarfs on the red side of the gap showing a large spread on lithium abundance and dwarfs located on the blue side showing low abundances. Given the dependence of the surface Li abundance on the thickness of the convective envelope, Kovtyukh et al. (2004) suggested a connection between this MS gap and convection.

4 CLUSTERS PARAMETERS

As we did in previous papers of this project, we derived the main clusters parameters using the synthetic CMD method, first described by Tosi et al. (1991). Tosi, Bragaglia & Cignoni (2007), Cignoni et al. (2011) and Donati et al. (2012) contain a recent, more extensive description of the procedure. We begin by building a library of artificial populations, Monte Carlo generated for different combinations of stellar age, metallicity, distance, Galactic reddening and binary fraction. The second step is compiling a list of CMD features useful to assess the likelihood between data and model CMDs. In order to make a meaningful comparison, all synthetic CMDs are combined with stars picked from an equal area of the adjacent comparison field, located away from the cluster centre. For each cluster, the synthetic CMD is populated until the total number of stars (synthetic plus field) equals the observed number of stars in the cluster field, and corrected for photometric errors and incompleteness, as derived from the artificial stars test. The obvious advantage of this procedure, with respect to the classical isochrone fitting technique, is the natural possibility of incorporating photometric errors, incompleteness and statistical fluctuations.

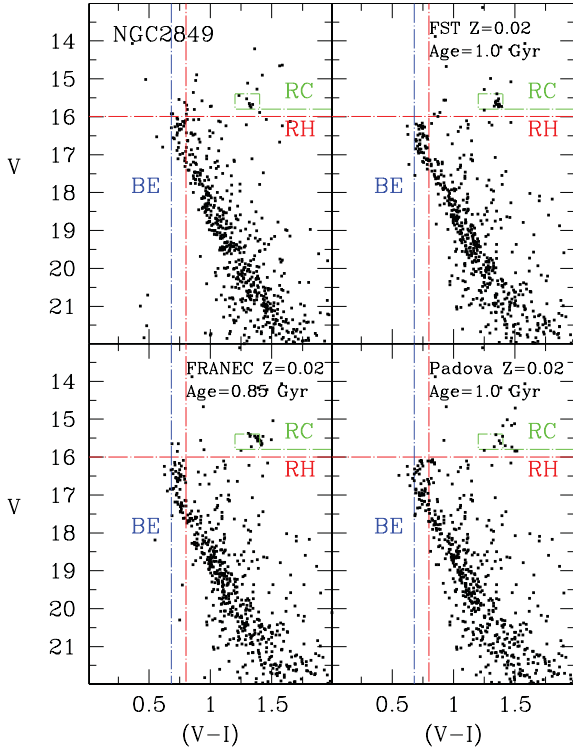


Figure 13. The upper-left panel shows the $V, V-I$ CMD for NGC 2849. The magnitude and colours of main evolutionary features are indicated with red (RH), green (RC) and blue (BE) dot-dashed lines. The other panels, clockwise from this, show the best-fitting synthetic CMDs for the following parameters: FST $Z = 0.02$, age 1.0 Gyr, $E(B-V) = 0.325 \pm 0.025$ and $(m-M)_0 = 13.8$; Padova $Z = 0.02$, age 1.0 Gyr, $E(B-V) = 0.285 \pm 0.025$ and $(m-M)_0 = 13.9$; FRANEC $Z = 0.02$, age 0.85 Gyr, $E(B-V) = 0.315 \pm 0.025$ and $(m-M)_0 = 13.95$. The adopted percentage of binaries (with random mass ratio) is always 30 per cent.

To minimize the subjectivity and take at least partially into account systematic effects, we use several sets of stellar tracks,⁴ namely the old Padova (Bressan et al. 1993; Fagotto et al. 1994), the Frascati Raphson Newton Evolutionary Code (FRANEC; Dominguez et al. 1999) and the FST ones (Ventura et al. 1998).

In order to lift or reduce the age–metallicity–reddening degeneracy, only those parameters that can actually reproduce the observed data in both $V, V-I$ and $V, B-V$ planes are considered acceptable solutions (see however Section 4.2).

4.1 NGC 2849

The OC NGC 2849 is intrinsically poorly populated and the high degree of field contamination makes it difficult to identify the cluster members. However, there are several features clearly visible in the CMD of Figs 8, 13 and 14 (showing the entire photometric data set):

- (i) An RC in the range $V = 15.4\text{--}15.8$. Its elongated shape suggests the presence of differential reddening.
- (ii) A hook-like structure, indicative of convective core TO stars, about 0.2 mag below the RC.

⁴ See Bragaglia & Tosi (2006) for a description of their main properties and a detailed justification of their use even if newer tracks have appeared in the meantime.

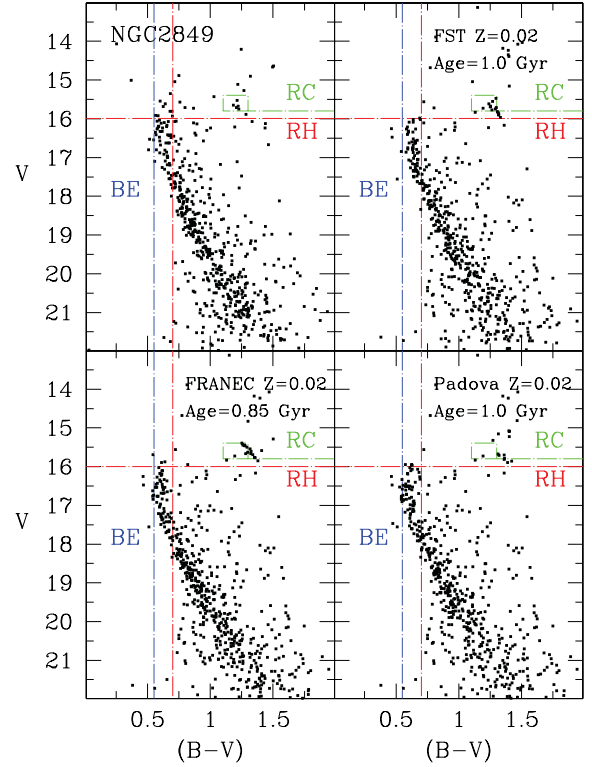


Figure 14. Same as in Fig. 13 but for the $V, B-V$ CMD.

- (iii) A rather sparse MS extending down to $V = 22$.
- (iv) A poorly developed red giant branch (RGB).

To help visualizing the data-model comparison, colour edges and magnitude levels of significant stellar phases are indicated on the observational CMD with lines of different colours: the bluest MS point (‘blue edge’, BE), the colour and luminosity of the reddest MS point (‘Red Hook’, RH) and bona fide RC stars.

Our simulations indicate that photometric errors and binaries alone cannot explain the MS width. A differential reddening $\Delta E(B-V)$ in the range $\sim 0.05\text{--}0.1$ mag would be enough to reproduce both the MS width and the RC shape. Given this uncertainty, the current data do not allow us to reach a firm conclusion about the binary fraction. Hence, we keep this parameter fixed at the ‘reasonable’ value – often found in past analyses – of 30 per cent. We try to fit simultaneously the colours of BE, RH and RC and the luminosities of RH and RC by adjusting the age, the foreground reddening and the distance modulus using tracks of different metallicities (solar metallicity and $Z = 0.004, 0.006, 0.008$ or 0.01 , depending on the set).

Of all the synthetic models, those with metallicity lower than solar show the larger discrepancies. First, it is not possible to fit at the same time the magnitude and colour differences between RC and TO stars. Secondly, the amount of reddening required to fit BE and RH colours in the $V, V-I$ plane is much lower (by about 0.1 mag) than required to match the same features in the $V, B-V$ plane. More in general, the synthetic CMDs show $B-V$ colours definitely too red for all cases when the $V-I$ colours are correct. We conclude that metallicities lower than $Z = 0.01$ are definitely ruled out, in contrast with the Kyeong et al. (2004) estimate ($[\text{Fe}/\text{H}] = -0.24 \pm 0.12$, or $Z \simeq 0.01$, obtained using the UV-excess).

Figs 13 and 14 show the best-match FST, PADOVA and FRANEC synthetic CMDs (clockwise from the top-right panel) computed for

solar metallicity. All models fit reasonably well both the $V, V - I$ and $V, B - V$ CMDs with approximately the same reddening. The only drawbacks are (i) the RC colour, which always appears slightly redder (and sparser for the Padova model) than the observational counterpart, probably suggesting a residual metallicity mismatch and (ii) the predicted number of RC stars, which outnumbers the observed one, by up to a factor of 2.

Our best estimate of the age of NGC 2849 is between 0.85 Gyr (FRANEC solution; models without overshooting always predict smaller values in this age range) and 1.00 Gyr (FST and PADOVA solutions). Both are slightly higher than the 0.6 Gyr found by Kyeong et al. (2004); however, their data are much shallower and the isochrone they chose does not seem to reproduce the RC.

The resulting total reddening⁵ is constrained between $E(B - V) = 0.285 \pm 0.025$ and $E(B - V) = 0.325 \pm 0.025$. These values are lower than what is obtained by the Schlegel, Finkbeiner & Davis (1998) maps; however, the latter ($E(B - V) \sim 0.44$) is actually an upper limit, being the asymptotic value in the given direction.

The derived distance modulus $[(m - M)_0 = 13.80\text{--}13.95]$ is in good agreement with Kyeong et al. (2004) and places the cluster at 640–680 pc over the Galactic plane, well beyond the thin disc height. This in turn explains the high differential reddening and the strong field contamination, since the line of sight intersects the Galactic disc for several kpc. Most of the field stars are foreground objects.

4.2 NGC 6134

The CMD of NGC 6134 is characterized by a well-defined MS, clearly visible down to about $V = 18\text{--}19$. The RC, which is the most prominent feature of the CMD, is at the same magnitude of the bluest point of the MS, suggesting an intermediate age. Few sparse RGB stars are also visible.

From the statistical point of view, NGC 6134 is more populous than NGC 2849, providing a better opportunity to compare data and models. Unfortunately, we cannot take full advantage of the external field because its CMD (see Fig. 10) is clearly different from the field contamination in NGC 6134's CMD, as already remarked in Section 3. While the NGC 6134 contamination shows a mildly visible RC population located 2–3 mag below the cluster RC and 1 mag to the right of the cluster MS, the comparison field CMD shows a clear stripe of RC stars running parallel to the MS, from $V = 14$ down to the completeness limit. Such a difference is intriguing because it contrasts with a standard thin disc model. NGC 6134's field is slightly closer to the Galactic plane; hence, its contamination was expected higher and more reddened than the external field's. A possible explanation may be that the reddening plane is tilted with respect to the Galactic plane. Indeed, Joshi (2005) finds that, around the Galactic longitude of NGC 6134, the plane defined by the reddening material might be inclined below the formal plane. In this way, the external field may be closer to the 'reddening plane' than NGC 6134's field and, therefore, affected by reddening for a longer distance. However it still remains difficult to explain why the external field is globally more populated.

As done for NGC 2849, the most relevant evolutionary phases are indicated with lines of different colours in Fig. 15. A visual inspection of the figure reveals a BE around $B - V \sim 0.57$, an

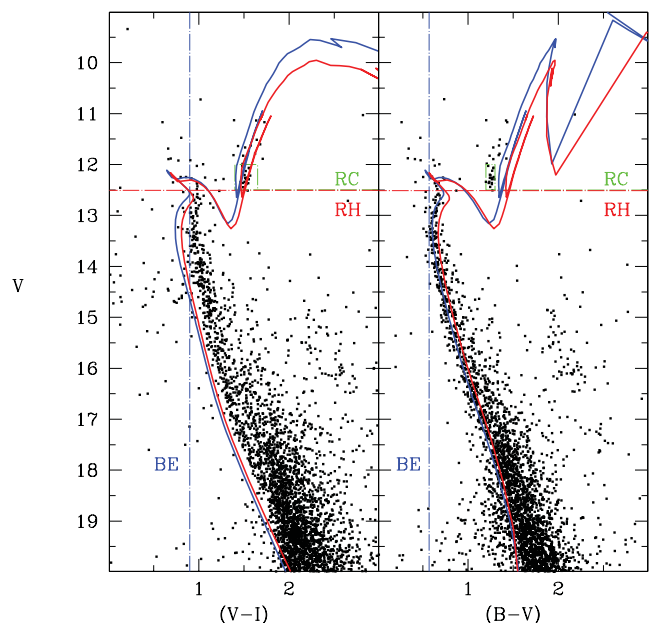


Figure 15. $V, V - I$ and $V, B - V$ for NGC 6134. The magnitude and colours of main evolutionary features follow the same nomenclature of Fig. 13. The solid lines show the Padova isochrones (Marigo et al. 2008) for 1 Gyr and $Z = 0.02$ (red) or $Z = 0.03$ (blue).

RH around $V \sim 12.5$ and $B - V \sim 0.57$ and a well-defined RC concentrated around $V = 12.25$.

It would seem an easy cluster to reproduce, also because its metallicity and reddening have been independently measured, see Carretta et al. (2004) and Section 4.2.1.1. Instead, no synthetic model for any of the three sets of tracks is able to simultaneously reproduce both the $B - V$ and $V - I$ colours of all the evolutionary phases. When models are tuned to fit the MS in $B - V$, the synthetic $V - I$ colours turn out to be systematically too blue. We also tried newer Padova isochrones (Marigo et al. 2008) with updated physical inputs and colour transformations, but the improvement is not significant (see Fig. 15). Moreover, the same effect is found also using a Bag of Stellar Tracks and Isochrones (BaSTI; e.g. Pietrinferni et al. 2004) and Victoria (VandenBerg, Bergbusch & Dowler 2006) sets of stellar models (the corresponding isochrones are not shown in the figure for clarity).

A similar problem had already been found for other clusters of the BOCCE project, including NGC 2849. However, in all those cases the mismatch was clearly a function of the assumed metallicity: larger for metallicities too different from the actual one, and increasingly small when approaching the right Z . In this case, the size of the discrepancy does not change with metallicity. We believe that the discrepancy can probably be attributed to the inability of past and present atmosphere models to reproduce real colours at high metallicity (i.e. low temperature), or, less probably, to a calibration issue with the I -magnitude (see below), or even less probably, to some difference in the reddening law towards this particular cluster. We further discuss this problem in Section 4.2.2.

Given the difficulty to define the metallicity and the reddening from the simultaneous fit of the $B - V$ and $V - I$ CMDs, we limited our analysis to constraining the age and distance of NGC 6134, assuming the spectroscopic abundance and the reddening derived from the $U - B$ versus $B - V$ diagram (see below). Then the most likely age and distance are determined by the simulated CMD which best fits the magnitude and colour difference between the RC and

⁵ Here the total reddening is the sum of a mean Galactic component and a random component ('differential') which includes the foreground fluctuation and a possible internal reddening.

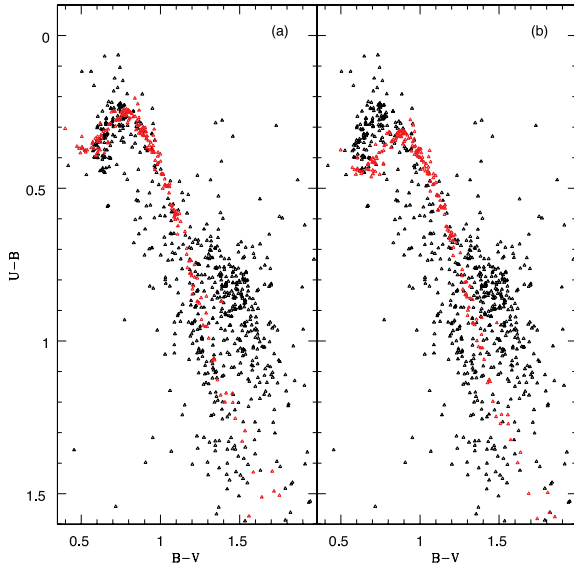


Figure 16. $U-B$, $B-V$ diagrams for NGC 6134 (black points in the online article) and the Hyades (red points in the online article). We plot stars with distances ≤ 4 arcmin from the cluster centre dereddened using two different colour excesses: $E(B-V) = 0.35$ (left-hand panel) and $E(B-V) = 0.45$ (right-hand panel). The fit is much better with the former value.

TO.⁶ We chose to use only the V , $B-V$ CMD for this computation. There is no guarantee that the colour transformations, if they truly are the culprits, work better in this colour. However, these are the filters we always have for all the BOCCE clusters, so we stick to them to maximize the homogeneity of treatment.

4.3 Reddening estimate

There is some dispersion in literature reddening values for NGC 6134 (see the introduction). Since, as already mentioned, the metallicity and age of the Hyades are similar, we compared our data with UBV photoelectric data from Johnson & Knuckles (1955) to derive a value for the reddening, using the two-colour diagram. In Fig. 16, we show the $B-V$, $U-B$ diagram for NGC 6134 stars with distances less than 4 arcmin from the centre (in black) and for the Hyades stars (red). The Hyades reddening is very low, $E(B-V) \leq 0.01$ (Taylor 2006). In Fig. 16, we dereddened our data using two values, $E(B-V) = 0.35$ and 0.45 , which represent the ones most commonly found in the literature. They correspond to $E(U-B) = 0.25$ and 0.32 , according to the relation $E(U-B)/E(B-V) = 0.70 + 0.05 E(B-V)$ (Fitzgerald 1970). The figure clearly shows that the lower reddening gives a much better fit, so it should be preferred. We note that this is also very close to the reddening derived by Carretta et al. (2004) in a totally independent way, based on spectroscopically determined temperatures and relations with intrinsic colours.

4.4 Best age and distance

For all simulations we assumed a fraction of binaries of 30 per cent and only the V , $B-V$ is used for the fit. The adopted metallicities are the closest to the spectroscopic value. Fig. 17 shows the best-fitting CMDs according to the FST (top-right panel), PADOVA (bottom-right panel) and FRANEC (bottom-left panel) models.

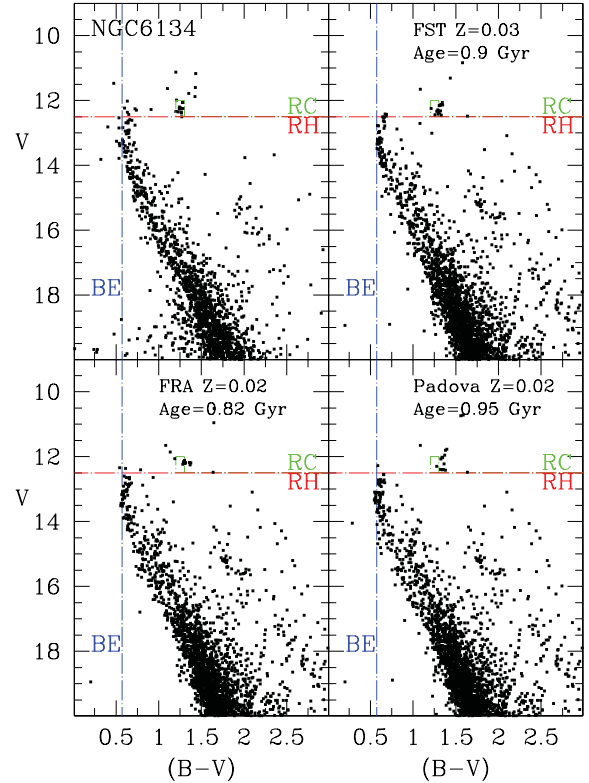


Figure 17. V , $B-V$ CMD for NGC 6134. The magnitude and colours of main evolutionary features follow the same nomenclature of Fig. 13. The other panels, clockwise from this, show the best-fitting synthetic CMDs for the following parameters: FST $Z = 0.03$, age 0.9 Gyr, $E(B-V) = 0.33$ and $(m-M)_0 = 10.5$; Padova $Z = 0.02$, age 0.95 Gyr, $E(B-V) = 0.33$ and $(m-M)_0 = 10.5$; FRANEC $Z = 0.02$, age 0.82 Gyr, $E(B-V) = 0.35$ and $(m-M)_0 = 10.5$. The adopted percentage of binaries (with random mass ratio) is always 30 per cent.

All simulations show a clear excess of field stars (both in the field RC region, below $V = 14$, and along the MS, below $V = 17$) as a direct consequence of the peculiar external field used to artificially contaminate our models. This should be disregarded. The cluster TO and the RC morphologies are well matched, while the slope of the MS is less reproduced. In terms of age, the best value is well constrained between 0.82 and 0.95 Gyr, in good agreement with Lindoff (1972), Clariá & Mermilliod (1992) and Kjeldsen & Frandsen (1991), but significantly younger than that found by Ahumada (2002). Overall, the reddening value inferred from the $U-B$, $B-V$ diagram works well, with no compelling evidence of differential reddening. The best distance modulus, $(m-M)_0 = 10.5$ (i.e. 1260 pc), places this cluster slightly farther than previously thought [700, 760, 912 and 1080 pc according to Lindoff (1972), Clariá & Mermilliod (1992), Kjeldsen & Frandsen (1991) and Ahumada (2002), respectively] and almost right on the Galactic plane.

4.5 OCs colours: a more general issue

Before discussing the possibility that all the considered evolutionary models are unable to consistently fit the observed CMDs in all colours, we need to exclude that there is a problem with our I photometry, since we had not met this problem for other BOCCE clusters. Unfortunately, no direct comparison with literature photometry is possible in this filter (see Section 2.3), so we took a

⁶ These differential features are less affected by reddening and metallicity.

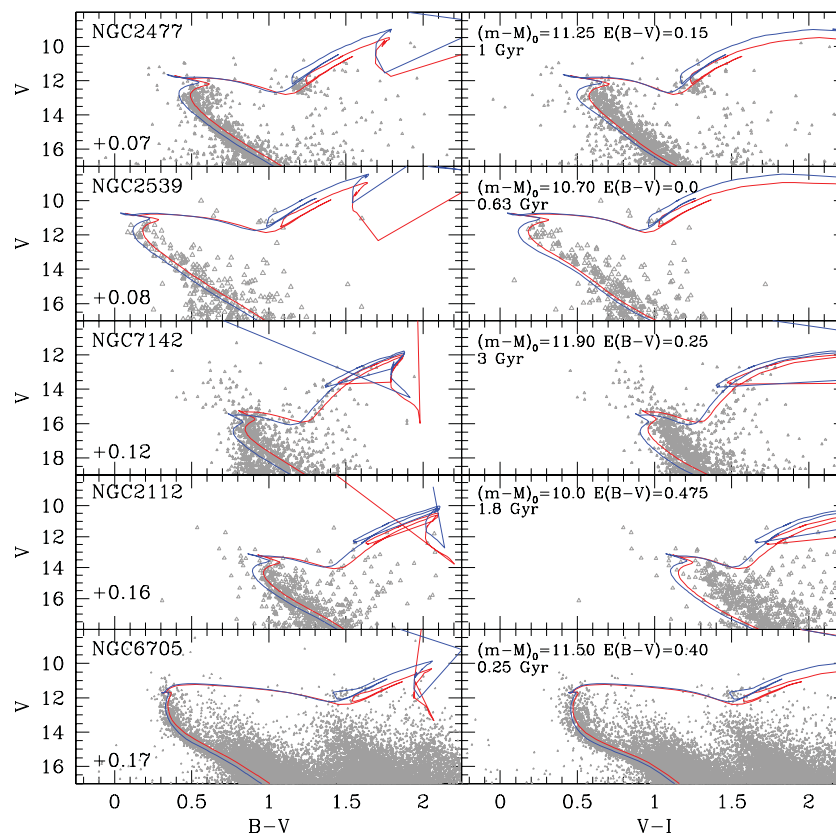


Figure 18. CMDs of five metal-rich OCs, $V, B - V$ on the left, $V, V - I$ on the right, with overimposed the best-fitting isochrones (see the text for details) in red (in the online article) and the solar ones in blue (in the online article).

more devious route. Suspecting that problems could arise at high metallicity, we selected other OCs of super-solar metallicity according to high-resolution spectroscopy and with B, V, I photometry available. We then compared data and models. Using the WEBDA, we finally selected five metal-rich OCs of different ages, namely NGC 2477, NGC 2539, NGC 7142, NGC 2112 and NGC 6705 (M11).⁷

Fig. 18 shows the $V, B - V$ (left-hand panels) and $V, V - I$ (right-hand panels) CMDs compared to the corresponding best-fitting Padova isochrones (obtained from the official website <http://stev.oapd.inaf.it/cmd>, see Marigo et al. 2008). The isochrones are taken already transformed from luminosity and temperature to magnitude and colour, at variance with what we usually do with the evolutionary tracks, where we apply our own transformations. The age is taken from the literature, while the metallicity is fixed at $Z = 0.03$ (red isochrones, but for comparison also solar isochrones are shown in blue). Distance and reddening are estimated by matching the $V, B - V$ CMD, while no attempt is done to fit the $V, V - I$ one (the relation $E(V - I) = 1.3 \times E(B - V)$ is used). This comparison highlights two important biases. First, *most* of these OCs exhibit the same problem observed in NGC 6134: when isochrones match well in $B - V$, they systematically fail in $V - I$, with the exception of NGC 6705. Second, in the $V, B - V$ CMDs most models deviate

systematically from the observed MS at faint magnitudes. Moreover, in some OCs the two biases may be at work simultaneously (see e.g. NGC 2112) and the oldest OCs (those with the coolest TOs) in the sample, NGC 2112 and NGC 7142, show the largest discrepancies. This may be a hint of an atmosphere issue.

One caveat to these results could be that the slightly different metallicity of each OC may account for a part of the mismatch. However, also the adoption of a solar metallicity (see the blue isochrones in Fig. 18) instead of $Z = 0.03$ does not change our conclusions. Given the similarity of results for the BaSTI and Victoria isochrones in the case of NGC 6134, we did not attempt a similar test with them, since it would be beyond the goal of our paper.

We also checked whether the same mismatches are present at sub-solar regimes. Again we selected clusters with metallicity based on high-resolution spectroscopy with BVI photometry available at the WEBDA (with all the three bands from the same source). Fig. 19 shows five representative examples, ordered in metallicity, with the metal-poorest at the top.⁸ Also in this case there appear to be a few mismatches, but they are much rarer and less pronounced. The oldest clusters (Be 17 and Be 39) are very well reproduced, as is the youngest one (NGC 2168), whilst in Be 29 and in NGC 2420 the fit in the two colours is not exactly the same. The reason for this is not straightforward: it cannot simply be metallicity (all these objects have about the same one) or age (both old, cool stars and young,

⁷ Their $[\text{Fe}/\text{H}]$ values are +0.07 (NGC 2477, Bragaglia et al. 2008); +0.08 (NGC 2539, Santos et al. 2009); +0.14 (NGC 7142, Jacobson, Friel & Pilachowski 2008); +0.16 (NGC 2121, Carraro et al. 2008); +0.17 (NGC 6705, Gonzalez & Wallerstein 2000). We did not attempt any homogenization of the metallicity scales, the only relevant information is that all these OCs have super-solar metal abundance.

⁸ Their $[\text{Fe}/\text{H}]$ values are -0.31 (Berkeley 29, Bragaglia et al. 2008); -0.20 (Berkeley 39, Bragaglia et al. 2012); -0.20 (NGC 2168, Barrado y Navascués, Deliyannis & Stauffer 2001); -0.10 (Berkeley 17, Friel, Jacobson & Pilachowski 2005); -0.05 (NGC 2420, Pancino et al. 2010).

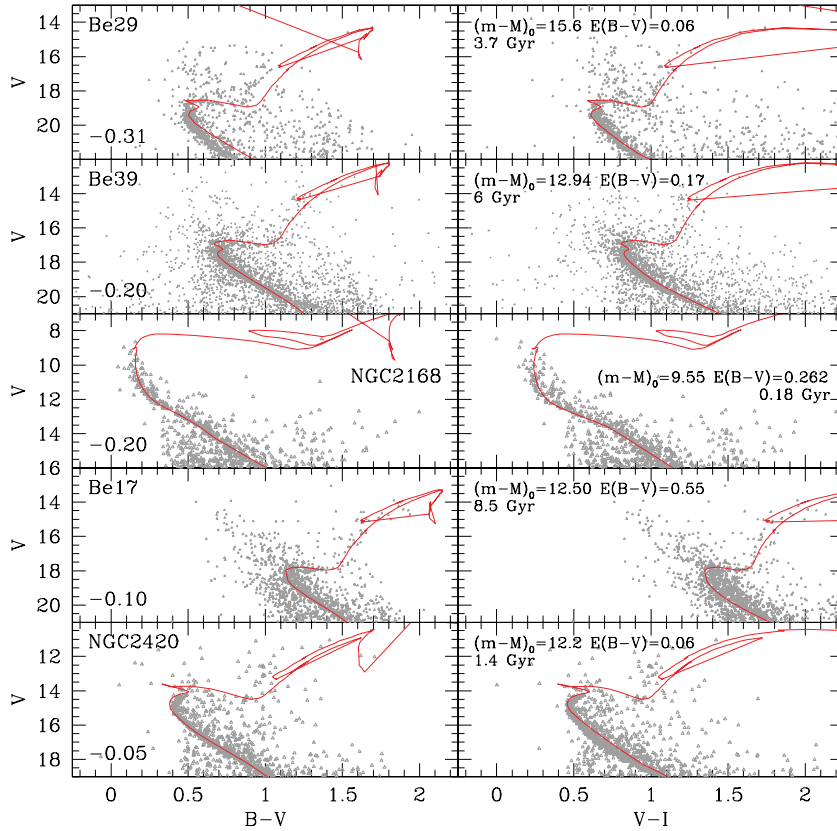


Figure 19. CMDs of five metal-poor OCs, $V, B - V$ on the left, $V, V - I$ on the right, with overimposed the best-fitting isochrones (see the text for details).

warm ones seem well fit by the isochrones). Maybe a difference in the metal mixture (e.g. different elemental ratios?) could be an explanation (see e.g. Gallart, Zoccali & Aparicio 2005). This problem requires further thorough investigations. When taken together these findings are a strong warning against any blind attempt to match the CMD without a multicolour analysis. Theoretical predictions will require a much firmer evaluation of colour–temperature relations.

5 SUMMARY AND CONCLUSIONS

In this work we have determined the evolutionary parameters of NGC 2849 and NGC 6134 by means of synthetic CMDs. From the comparison between models and data we have drawn the following conclusions.

(i) The most likely metallicity for NGC 2849 is above $Z = 0.01$. Of all the synthetic models, only those with metallicity $Z = 0.02$ are able to simultaneously reproduce both the $B - V$ and $V - I$ colours of all the evolutionary phases. Concerning the age, our best estimate is between 0.85 (FRANEC solution) and 1.00 Gyr (FST and PADOVA solutions), while the distance modulus and reddening $E(B - V)$ are constrained in the range 13.8–13.95 (5750–6170 pc) and 0.28–0.32, respectively.

(ii) Even though NGC 6134 is almost identical in age and reddening to NGC 2849, fitting its CMD has posed serious difficulties, chiefly connected with colours. In fact, none of our models is able to simultaneously reproduce both the $B - V$ and $V - I$ colours of all the evolutionary phases, making it impossible to estimate the cluster reddening and metallicity. In order to verify if this problem illustrates a more general difficulty of synthetic stellar atmospheres, we have extended our analysis to five metal-rich and to five metal-poor

OCs taken from the WEBDA data base, with precise metallicity determination. We found similar discrepancies which are more pronounced for the rich ones. We suspect a difference in the metal mixture assumed by the models and those of the clusters.

(iii) Given these difficulties we have built all synthetic CMDs using the spectroscopic abundance $[Fe/H] = 0.15 \pm 0.03$; Carretta et al. 2004) and the reddening value inferred from the $U - B, B - V$ plot $[E(B - V) = 0.35]$. With these assumptions we have recovered for NGC 6134 a best-fitting age between 0.82 and 0.95 Gyr and a distance modulus 10.5 (1260 pc).

(iv) Besides these features, NGC 6134's CMD shows a *striking MS gap* around $B - V \sim 0.9$ – 1.0 which had already been noted by Kjeldsen & Frandsen (1991). Similar gaps have been observed in other OCs without clear correlation with age and metallicity. Although convection may offer an explanation for some of them, this is a research area where new models are needed.

(v) We remark once more the interesting morphology of the comparison field of NGC 6134. Here the RC is very elongated and the overall CMD is more populated than expected, thus suggesting a peculiar reddening distribution or an additional Galactic population in this direction.

A new era for OCs is coming soon with the ESA mission *Gaia*⁹ and some ground-based, spectroscopic surveys, like APOGEE¹⁰, the HERMES Project¹¹ (High Efficiency and Resolution Multi-Element Spectrograph for the AAT) and GES¹² (*Gaia*-ESO Survey) which

⁹ gaia.esa.int

¹⁰ <http://www.sdss3.org/surveys/apogee.php>

¹¹ <http://www.aao.gov.au/HERMES/>

¹² <http://www.gaia-eso.eu>

will observe in the IR or optical wavelengths hundreds of OCs, covering all accessible cluster ages and stellar masses. The GES, in particular, just started and employed FLAMES at the VLT, will be able to reach also very far clusters and/or obtain spectra for many MS stars. With this information, coupled with *Gaia* distances and proper motions, it will be possible to better characterize and understand the Galactic OC population.

ACKNOWLEDGMENTS

We thank the referee for the useful and constructive comments that helped to improve the paper. This research has made use of NASA's Astrophysics Data System, the SIMBAD data base (operated at CDS, Strasbourg, France), the facilities of the Canadian Astronomy Data Centre (operated by the National Research Council of Canada with the support of the Canadian Space Agency), the WEBDA data base (operated at the Institute for Astronomy of the University of Vienna), the SAOImage DS9, developed by Smithsonian Astrophysical Observatory, the Digitized Sky Survey (DSS was produced at the Space Telescope Science Institute under U.S. Government grant NAG W-2166. The images of these surveys are based on photographic data obtained using the Oschin Schmidt Telescope on Palomar Mountain and the UK Schmidt Telescope. The plates were processed into the present compressed digital form with the permission of these institutions), and the Guide Star Catalogue-II (GSC II is a joint project of the Space Telescope Science Institute) and the Osservatorio Astronomico di Torino. We thank Paolo Montegriffo (OABO, Osservatorio Astronomico di Bologna, Italy) for his software CataPack. AVA thanks for hospitality the OABO, where this paper was written and Gabriele Coccozza (OABO) for his kind help with data reduction.

REFERENCES

- Ahumada J. A., 2002, in Lejeune T., Fernandes J., eds, *Observed HR Diagrams and Stellar Evolution*, ASP Conf. Ser. Vol. 274, Astron. Soc. Pac., San Francisco, p. 307
- Ahumada J. A., 2003, *Rev. Mex. Astron. Astrofis.*, 39, 41
- Balaguer-Núñez L., Jordi C., Galadí-Enríquez D., 2005, *A&A*, 437, 457
- Barrado y Navascués D., Deliyannis C. P., Stauffer J. R., 2001, *ApJ*, 549, 452
- Böhm-Vitense E., 1995, *AJ*, 110, 228
- Bragaglia A., Tosi M., 2006, *AJ*, 131, 1544
- Bragaglia A. et al., 2001, *AJ*, 121, 327
- Bragaglia A., Tosi M., Carretta E., Gratton R. G., Marconi G., Pompei E., 2006, *MNRAS*, 366, 1493
- Bragaglia A., Sestito P., Villanova S., Carretta E., Randich S., Tosi M., 2008, *A&A*, 480, 79
- Bragaglia A., Carretta E., D'Orazi V., Gratton R. G., Sneden C., Lucatello S., 2012, *A&A*, in press
- Bressan A., Fagotto F., Bertelli G., Chiosi C., 1993, *A&AS*, 100, 647
- Bruntt H., Frandsen S., Kjeldsen H., Andersen M. I., 1999, *A&AS*, 140, 135
- Carraro G., Villanova S., Demarque P., Moni Bidin C., McSwain M. V., 2008, *MNRAS*, 386, 1625
- Carretta E., Bragaglia A., Gratton R., Tosi M., 2004, *A&A*, 422, 951
- Cignoni M., Tosi M., Bragaglia A., Kalirai J. S., Davis D. S., 2008, *MNRAS*, 386, 2235
- Cignoni M., Beccari G., Bragaglia A., Tosi M., 2011, *MNRAS*, 416, 1077
- Clariá J. J., Mermilliod J.-C., 1992, *A&AS*, 95, 429
- Collinder P., 1931, *Ann. Obs. Lund*, 2, 1
- Cousins A. W. J., Caldwell J. A. R., 1985, *The Observatory*, 105, 134
- D'Antona F., Montalbán J., Kupka F., Heiter U., 2002, *ApJ*, 564, L93
- de Bruijne J. H. J., Hoogerwerf R., de Zeeuw P. T., 2000, *ApJ*, 544, L65
- Dominguez I., Chieffi A., Limongi M., Straniero O., 1999, *ApJ*, 524, 226
- Donati P., Bragaglia A., Cignoni M., Coccozza G., Tosi M., 2012, *MNRAS*, 424, 1132
- Fagotto F., Bressan A., Bertelli G., Chiosi C., 1994, *A&AS*, 105, 29
- Fitzgerald M. P., 1970, *A&A*, 4, 234
- Frandsen S., Balona L. A., Viskum M., Koen C., Kjeldsen H., 1996, *A&A*, 308, 132
- Friel E. D., 1995, *ARA&A*, 33, 381
- Friel E. D., Janes K. A., Tavaréz M., Scott J., Katsanis R., Lotz J., Hong L., Miller N., 2002, *AJ*, 124, 2693
- Friel E. D., Jacobson H. R., Pilachowski C. A., 2005, *AJ*, 129, 2725
- Friel E. D., Jacobson H. R., Pilachowski C. A., 2010, *AJ*, 139, 1942
- Gallart C., Zoccali M., Aparicio A., 2005, *ARA&A*, 43, 387
- Gilmore G. et al., 2012, *Messenger*, 147, 25
- Giorgi E. E., Vázquez R. A., Baume G., Seggewiss W., Will J.-M., 2002, *A&A*, 381, 884
- Gonzalez G., Wallerstein G., 2000, *PASP*, 112, 1081
- Jacobson H. R., Friel E. D., Pilachowski C. A., 2008, *AJ*, 135, 2341
- Johnson H. L., Knuckles C. F., 1955, *ApJ*, 122, 209
- Joshi Y. C., 2005, *MNRAS*, 362, 1259
- Kjeldsen H., Frandsen S., 1991, *A&AS*, 87, 119
- Kovtyukh V. V., Soubiran C., Belik S. I., 2004, *A&A*, 427, 933
- Kyeong J.-M., Byun Y.-I., Sung E.-C., Chun M.-S., 2004, *AJ*, 128, 2331
- Landolt A., 1992, *AJ*, 104, 340
- Lauberts A., 1982, *The ESO/Uppsala Survey of the ESO (B) Atlas*, European Southern Observatory, Garching
- Lépine J. R. D. et al., 2011, *MNRAS*, 417, 698
- Lindoff U., 1972, *A&AS*, 7, 231
- Lyngå G., 1987, *Lund Catalogue of Open Cluster Data*, 5th edn., CDS, Strasbourg
- Majewski S. R., 2012, *American Astronomical Society, AAS Meeting*, #219, #205.06
- Marigo P., Girardi L., Bressan A., Groenewegen M. A. T., Silva L., Granato G. L., 2008, *A&A*, 482, 883
- Melotte P. J., 1915, *Mem. R. Astron. Soc.*, 60, 181
- Mikolaitis S., Tautvaisiene G., Gratton R., Bragaglia A., Carretta E., 2010, *MNRAS*, 407, 1866
- Pancino E., Carrera R., Rossetti E., Gallart C., 2010, *A&A*, 511, A56
- Paunzen E., Maitzen H. M., 2002, *A&A*, 385, 867
- Pietrinferni A., Cassisi S., Salaris M., Castelli F., 2004, *ApJ*, 612, 168
- Rasmussen M. B., Bruntt H., Frandsen S., Paunzen E., Maitzen H. M., 2002, *A&A*, 390, 109
- Santos N. C., Lovis C., Pace G., Melendez J., Naef D., 2009, *A&A*, 493, 309
- Schlegel D. J., Finkbeiner D. P., Davis M., 1998, *ApJ*, 500, 525
- Sestito P., Bragaglia A., Randich S., Pallavicini R., Andrievsky S. M., Korotin S. A., 2008, *A&A*, 488, 943
- Smiljanic R., Gauderon R., North P., Barbuy B., Charbonnel C., Mowlavi N., 2009, *A&A*, 502, 267
- Stetson P. B., 1987, *PASP*, 99, 191
- Stetson P. B., 1993, in Butler C. J., Elliott I., eds, *Stellar photometry - Current techniques and future developments*, Proc. IAU Colloquium 136, Cambridge Univ. Press, Cambridge, p. 291
- Subramaniam A., Bhatt B. C., 2007, *MNRAS*, 377, 829
- Taylor B. J., 2006, *AJ*, 132, 2453
- Tosi M., Greggio L., Marconi G., Focardi P., 1991, *AJ*, 102, 951
- Tosi M., Di Fabrizio L., Bragaglia A., Carusillo P. A., Marconi G., 2004, *MNRAS*, 354, 225
- Tosi M., Bragaglia A., Cignoni M., 2007, *MNRAS*, 378, 730
- Twarog B., Ashman K., Anthony-Twarog B. J., 1997, *AJ*, 114, 2556
- van den Bergh S., Hagen G. L., 1975, *AJ*, 80, 11
- VandenBerg D. A., Bergbusch P. A., Dowler P. D., 2006, *ApJS*, 162, 375
- Ventura P., Zepieri A., Mazzitelli I., D'Antona F., 1998, *A&A*, 334, 953
- Wu Z.-Y., Zhou X., Ma J., Du C.-H., 2009, *MNRAS*, 309, 2146
- Yong D., Carney B. W., Friel E. D., 2012, *AJ*, 144, 95